http://dx.doi.org/10.5012/bkcs.2013.34.11.3218

Kinetics and Mechanism of the Aminolyses of Bis(2-oxo-3-oxazolidinyl) Phosphinic Chloride in Acetonitrile

Hasi Rani Barai and Hai Whang Lee*

*Department of Chemistry, Inha University, Incheon 402-751, Korea. *E-mail: hwlee@inha.ac.kr*
Received July 29, 2013, Accepted August 5, 2013

The aminolyses, anilinolysis and pyridinolysis, of bis(2-oxo-3-oxazolidinyl) phosphinic chloride (**1**) have been kinetically investigated in acetonitrile at 55.0 and 35.0 °C, respectively. For the reactions of **1** with substituted anilines and deuterated anilines, a concerted S_N2 mechanism is proposed based on the selectivity parameters and activation parameters. The deuterium kinetic isotope effects (k_H/k_D) invariably increase from secondary inverse to primary normal as the aniline becomes more basic, rationalized by the transition state variation from a backside to a frontside attack. For the pyridinolysis of **1**, the authors propose a stepwise mechanism with a rate-limiting step change from bond breaking for more basic pyridines to bond formation for less basic pyridines based on the selectivity parameters and activation parameters. Biphasic concave upward free energy relationship with X is ascribed to a change in the attacking direction of the nucleophile from a frontside attack with more basic pyridines to a backside attack with less basic pyridines.

Key Words : Phosphoryl transfer reaction, Anilinolysis, Pyridinolysis, Bis(2-oxo-3-oxazolidinyl) phosphinic chloride, Deuterium kinetic isotope effect

Introduction

Continuing the kinetic studies on the aminolyses of $(Lig_1)(Lig_2)P(=O$ or $=S)Cl$-type substrates, the reactions of bis(2-oxo-3-oxazolidinyl) phosphinic chloride (**1**) with anilines [$XC_6H_4NH_2(D_2)$] and pyridines (XC_5H_4N) are examined in acetonitrile (MeCN) at 55.0 ± 0.1 and 35.0 ± 0.1 °C (Schemes 1 and 2), respectively. The purpose of this work is to gain further information on the phosphoryl transfer reactions regarding the selectivity parameters, deuterium kinetic isotope effects (DKIEs), activation parameter and steric effects of the two ligands.

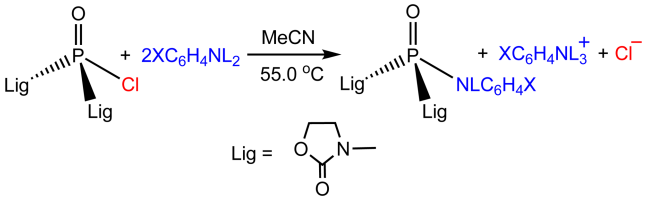

Scheme 1. Anilinolysis of bis(2-oxo-3-oxazolidinyl) phosphinic chloride (**1**) in MeCN at 55.0 °C.

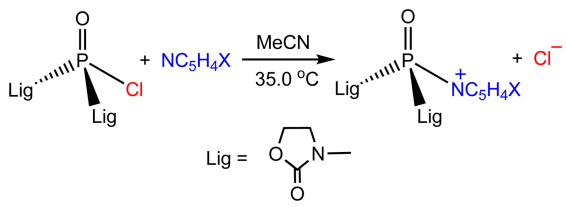

Scheme 2. Pyridinolysis of bis(2-oxo-3-oxazolidinyl) phosphinic chloride (**1**) in MeCN at 35.0 °C.

Results and Discussion

The second-order rate constants (k_H and k_D) of the anilinolysis in MeCN at 55.0 °C are summarized in Table 1, together with the Hammett ρ_X (Fig. S1) and Brönsted β_X (Fig. 1) selectivity parameters and DKIEs (k_H/k_D). The stronger nucleophile leads to the faster rate as observed in a typical nucleophilic substitution reaction with positive charge development at the nucleophilic N atom in the transition state (TS). The magnitudes of the $\rho_{X(H)}$ (= –3.23) and $\beta_{X(H)}$ (= 1.14) values with anilines are somewhat larger than those ($\rho_{X(D)}$ = –2.61 and $\beta_{X(D)}$ = 0.92) with deuterated aniline, suggesting more sensitive to substituent effects of the anilines compared to those of deuterated anilines. The

Table 1. Second-Order Rate Constants ($k_{H(D)} \times 10^4/M^{-1}\,s^{-1}$), Selectivity Parameters (ρ_X and β_X) and DKIEs (k_H/k_D) of the Reactions of Bis(2-oxo-3-oxazolidinyl) Phosphinic Chloride (**1**) with $XC_6H_4NH_2(D_2)$ in MeCN at 55.0 °C

X	$k_H \times 10^4$	$k_D \times 10^4$	k_H/k_D
4-MeO	61.9 ± 0.1	39.4 ± 0.1	1.57 ± 0.01[e]
4-Me	26.0 ± 0.2	22.5 ± 0.1	1.16 ± 0.01
3-Me	11.6 ± 0.1	12.0 ± 0.1	0.967 ± 0.012
H	7.05 ± 0.01	7.86 ± 0.03	0.897 ± 0.004
4-F	4.52 ± 0.02	5.58 ± 0.01	0.810 ± 0.004
3-MeO	3.38 ± 0.01	4.30 ± 0.01	0.786 ± 0.003
4-Cl	1.30 ± 0.01	2.01 ± 0.01	0.647 ± 0.006
3-Cl	0.507 ± 0.004	0.827 ± 0.001	0.613 ± 0.001
	$\rho_{X(H)} = -3.23 \pm 0.04$[a]	$\rho_{X(D)} = -2.61 \pm 0.02$[c]	
	$\beta_{X(H)} = 1.14 \pm 0.08$[b]	$\beta_{X(D)} = 0.92 \pm 0.05$[d]	

[a]Correlation coefficient, r = 0.999. [b]r = 0.994. [c]r = 0.999. [d]r = 0.996. [e]Standard error $\{= 1/k_D[(\Delta k_H)^2 + (k_H/k_D)^2 \times (\Delta k_D)^2]^{1/2}\}$.

Table 2. Second-Order Rate Constants ($k_{Pyr} \times 10^4/M^{-1}\ s^{-1}$) of the Reactions of Bis(2-oxo-3-oxazolidinyl) Phosphinic chloride (**1**) with XC_5H_4N in MeCN at 35.0 °C

X	4-MeO	4-Me	3-Me	H	3-Ph	3-MeO	3-Cl	3-Ac	4-Ac	3-CN	4-CN
k_{Pyr} $\times 10^4$	1050 ± 10	132 ± 2	16.8 ± 0.1	3.76 ± 0.01	3.16 ± 0.01	2.68 ± 0.02	1.28 ± 0.01	1.24 ± 0.01	0.818 ± 0.001	0.669 ± 0.001	0.511 ± 0.005

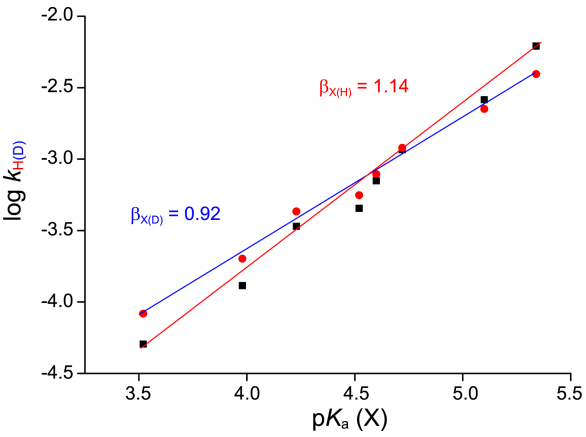

Figure 1. Brönsted plot of the reactions of bis(2-oxo-3-oxazolidinyl) phosphinic chloride (**1**) with $XC_6H_4NH_2(D_2)$ in MeCN at 55.0 °C.

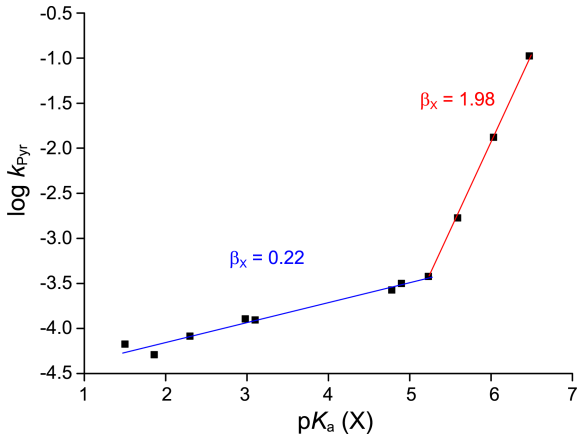

Figure 2. Brönsted plot of the reactions of bis(2-oxo-3-oxazolidinyl) phosphinic chloride (**1**) with X-pyridines in MeCN at 35.0 °C.

magnitudes of k_H/k_D values invariably decrease from the primary normal DKIEs (k_H/k_D = 1.57-1.16 > 1) with X = (4-MeO, 4-Me) to the secondary inverse DKIEs (k_H/k_D = 0.97-0.61 < 1) with X = (3-Me, H, 4-F, 3-MeO, 4-Cl, 3-Cl) as the aniline becomes less basic. Table 2 summarizes the second-order rate constants (k_{Pyr}) of the pyridinolysis in MeCN at 35.0 °C. The substituent effects of the nucleophiles upon the pyridinolysis rates also correlate with those for a typical nucleophilic substitution reaction. Both the Hammett (Fig. S2) and Brönsted (Fig. 2) plots, however, are biphasic concave upwards with a break point at X = H. The magnitudes of the ρ_X (= –9.05 ± 0.01; r = 0.999) and β_X (= 1.98 ± 0.04; r = 0.999) values with more basic pyridines (X = 4-MeO, 4-Me, 3-Me, H) are much greater than those [ρ_X = –1.33 ± 0.04 (r = 0.999) and β_X = 0.22 ± 0.06 (r = 0.985)] with less basic pyridines (X = H, 3-Ph, 3-MeO, 3-Cl, 3-Ac, 4-Ac, 3-CN, 4-CN).

Table 3 summarizes the second-order rate constants (k_H) with unsubstituted aniline ($C_6H_5NH_2$), Brönsted coefficients ($\beta_{X(H)}$), cross-interaction constant (CIC, $\rho_{XY(H)}$),[1] enthalpies ($\Delta H^{\ddagger}$/kcal mol^{-1}) and entropies ($\Delta S^{\ddagger}$/cal mol^{-1} K^{-1}) of activation with unsubstituted aniline, and DKIEs (k_H/k_D) of the reactions of **1** and **2** (Y-aryl phenyl chlorophosphate)[2] with $XC_6H_4NH_2(D_2)$ in MeCN at 55.0 °C. The authors reported that the steric effects (over the inductive effects) of the two ligands are the major factor to determine the anilinolysis rates: the larger the two ligands, the steric effects become greater in the TS, and the rate becomes slower.[3] The size of 2-oxo-3-oxazolidinyl in **1** is smaller than that of PhO in **2**. The anilinolysis rate ($C_6H_5NH_2$) of **1** is more or less slower than that of **2** with Y = H [$(PhO)_2P(=O)Cl$]; the ratio of k_H(**2** with Y = H)/k_D(**1**) = 1.26. At a glance, the kinetic results are not in line with expectation for the steric effects of the two ligands. Taking into account the structure difference between **1** and **2**, the presence of the oxygen atom between phenyl ring and reaction center phosphorus in **2** would render more available space to aniline nucleophile compared to **1** where the five-membered ring is directly bonded to reaction center P. Thus, the rate of **2** is somewhat faster than that of **1** in spite of the larger size of the phenoxy ligand compared to that of the 2-oxo-3-oxazolidinyl ligand. In other words, the steric congestion due to the two 2-oxo-3-oxazolidinyl ligands in **1** is somewhat greater than that due to the two phenoxy ligands in **2** in the TS. The value of $\beta_{X(H)}$ (= 1.14) of **1** is slightly smaller than that of **2** ($\beta_{X(H)}$ = 1.36 with Y = H).[2] The activation parameters, determined for the anilinolysis (with

Table 3. Summary of the Second-Order Rate Constants ($k_H \times 10^4/M^{-1}\ s^{-1}$) with $C_6H_5NH_2$, Brönsted Coefficients ($\beta_{X(H)}$), CIC ($\rho_{XY(H)}$), Enthalpies ($\Delta H^{\ddagger}$/kcal mol^{-1}) and Entropies ($\Delta S^{\ddagger}$/e.u.) of Activation with $C_6H_5NH_2$, and DKIEs (k_H/k_D) for the Reactions of **1** and **2** with $XC_6H_4NH_2(D_2)$ in MeCN at 55.0 °C

substrate	$10^4 k_H{}^a$	$\beta_{X(H)}$	$\rho_{XY(H)}$	$\Delta H^{\ddagger a}$	$-\Delta S^{\ddagger a}$	k_H/k_D
1: [*c*-$C_2H_2OC(=O)N]_2P(=O)Cl$	7.05	1.14	–	9.7[c]	44[c]	0.61-1.57
2: $(PhO)(YC_6H_4O)P(=O)Cl$	8.91[b]	1.24-1.68	–1.31	9.7[b]	43[b]	0.61-0.87

[a]Value with unsubstituted aniline (X = H). [b]Value with Y = H. [c]See Table S1 in Supporting Information.

$C_6H_5NH_2$) of **1** and **2**, are quite similar. The enthalpies of activation are relatively low ($\Delta H^{\ddagger}$ = 9.7 kcal mol^{-1} with both **1** and **2**) and entropies of activation are relatively large negative values ($\Delta S^{\ddagger}$ = –44 and –43 cal mol^{-1} K^{-1} with **1** and **2**, respectively). In general, the relatively low activation enthalpy and large negative activation entropy are typical for the aminolyses of phosphoryl transfer reactions.

The DKIEs can be only secondary inverse (k_H/k_D < 1) in a normal S_N2 reaction, because the N–H(D) vibrational frequencies invariably increase upon going to the TS (*e.g.*, in-line-type TSb in Scheme 3; backside attack), given the increase in steric hindrance in the bond formation step.[4] In contrast, when partial deprotonation of the aniline occurs in a rate-limiting step by hydrogen bonding (*e.g.*, hydrogen-bonded, four-center-type TSf in Scheme 2; frontside attack), the DKIEs are primary normal (k_H/k_D > 1).[5] The variation trends of k_H/k_D values with X of **1** and **2** are the same; the stronger the aniline, the k_H/k_D values becomes larger. A backside attack TSb was proposed for the anilinolysis of **2** based on the secondary inverse DKIEs, k_H/k_D = 0.61-0.87.[2] In the present work, the authors propose that the attacking direction of aniline toward the reaction center P atom changes from predominant frontside attack involving hydrogen bonded, four-center-type TSf with stronger anilines (X = 4-MeO, 4-Me) based on the primary normal DKIEs (k_H/k_D = 1.16-1.57) to dominant backside attack involving in-line-type TSb with weaker anilines (X = 3-Me, H, 4-F, 3-MeO, 4-Cl, 3-Cl) based on the secondary inverse DKIEs (k_H/k_D = 0.61-0.97). These can be rationalized by the gradual TS variation from a frontside to a backside attack as the aniline becomes less basic. The considerably small value of k_H/k_D = 0.61 with X = 3-Cl suggests severe steric hindrance, whereas the relatively large value of k_H/k_D = 1.57 with X = 4-MeO suggests the extensive hydrogen bonding in the TS.

A concerted mechanism was proposed based on the negative ρ_{XY} (= –1.31) value for the anilinolysis of **2**.[2] In the present work of **1**, a concerted mechanism is proposed based on: (i) the Brönsted coefficient of $\beta_{X(H)}$(**1**) = 1.14 is comparable with $\beta_{X(H)}$(**2**) = 1.24-1.68; (ii) the activation parameters of **1** ($\Delta H^{\ddagger}$ = 9.7 kcal mol^{-1} and $\Delta S^{\ddagger}$ = –44 cal mol^{-1} K^{-1}) are quite similar to those of **2** ($\Delta H^{\ddagger}$ = 9.7 kcal mol^{-1} and $\Delta S^{\ddagger}$ = –43 cal mol^{-1} K^{-1}); and (iii) the same variation trends of the DKIEs with X of **1** and **2**, where the magnitude of k_H/k_D increases with a stronger aniline.

The second-order rate constants (k_{Pyr}) with unsubstituted pyridine at 35.0 °C, Brönsted coefficients (β_X), CICs (ρ_{XY}), enthalpies ($\Delta H^{\ddagger}$/kcal mol^{-1}) and entropies ($\Delta S^{\ddagger}$/cal mol^{-1} K^{-1}) of activation with C_5H_5N for the pyridinolyses of **1**, **2**[6] and **2S** (Y-aryl phenyl chlorothiophosphate)[7] in MeCN are summarized in Table 4. The pyridinolysis rate of **2** is much faster than that of **1**; k_{Pyr}(**2**)/k_{Pyr}(**1**) = 707 at 35.0 °C.[8] This strongly suggests that the pyridinolysis mechanism of **2** is different from that of **1**. A concerted mechanism with very early TS was proposed for the pyridinolysis of **2**, in which the extent of both bond formation and leaving group departure is small, based on the small β_X (= 0.16-0.18) and small negative CIC (ρ_{XY} = –0.15).[1,6] The pyridinolysis rate of **2S** is relatively slow due to the so-called "thio effect", which is mainly the electronegativity difference between O and S and favors P=O over P=S.[9] In the pyridinolysis of **2S**, four different values of ρ_{XY} are available because both Hammett plots for substituent X and Y variations are biphasic with a break point. A stepwise mechanism with a rate-limiting leaving group departure from the intermediate was proposed for *a*-block (stronger nucleophiles and weaker electrophiles) and *b*-block (weaker nucleophiles and weaker electrophiles) based on the positive sign of ρ_{XY}, while a stepwise process with a rate-limiting bond formation was proposed for *c*-block (stronger nucleophiles and stronger electrophiles) and *d*-block (weaker nucleophiles and stronger electrophiles) based on the negative sign of ρ_{XY}.[7,10] The nonlinear

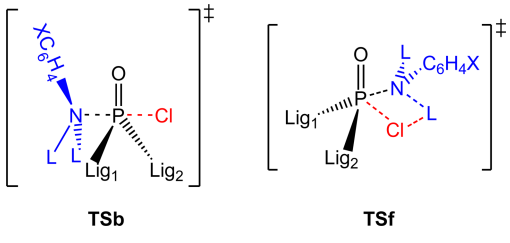

Scheme 3. Backside attack involving in-line-type TSb and frontside attack involving hydrogen-bonded, four-center-type TSf (L = H or D). Lig_1 and Lig_2 represent the two ligands.

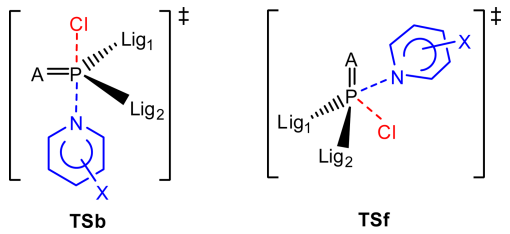

Scheme 4. Backside attack TSb and frontside attack TSf (A = O or S).

Table 4. Summary of the Second-Order Rate Constants (k_{Pyr} × 10^4/M^{-1} s^{-1}) with C_5H_5N, Brönsted Coefficients (β_X), CICs (ρ_{XY}), Enthalpies ($\Delta H^{\ddagger}$/kcal mol^{-1}) and Entropies ($\Delta S^{\ddagger}$/e.u.) of Activation with C_5H_5N for the Reactions of **1**, **2** and **2S** with XC_5H_4N in MeCN

substrate	10^4k_{Pyr}[a]	β_X	ρ_{XY}	$\Delta H^{\ddagger}$	$-\Delta S^{\ddagger}$
1: [*c*-$C_2H_2OC(=O)N]_2P(=O)Cl$	3.76	1.98/0.22[d]	–	3.5[g]	63[g]
2: $(PhO)(YC_6H_4O)P(=O)Cl$	2660[b,c]	0.16-0.18[e]	–0.15[e]	10.2	28
2S: $(PhO)(YC_6H_4O)P(=S)Cl$	0.333[b]	1.36-1.50/0.23-0.48[d]	2.42/5.14/–1.02/–0.04[f]	6.4	53

[a]Value with unsubstituted pyridine (X = H) at 35.0 °C. [b]Value with Y = H. [c]Value of k_{Pyr} = 2660 × 10^{-4} M^{-1} s^{-1} at 35.0 °C is an extrapolated value in the Arrhenius plot with kinetic data: k_{Pyr} = 371, 940, and 1350 × 10^{-4} M^{-1} s^{-1} at 5.0, 15.0 and 25.0 °C, respectively. [d]More/less basic pyridines at 35.0 °C. [e]Value at 25.0 °C. [f]*a*-block(stronger nucleophiles and weaker electrophiles)/*b*-block(weaker nucleophiles and weaker electrophiles)/*c*-block(stronger nucleophiles and stronger electrophiles)/*d*-block(weaker nucleophiles and stronger electrophiles). [g]See Table S2 in Supporting Information.

free energy correlations of biphasic concave upward plots with X were rationalized by a change in the attacking direction of the nucleophile from a backside (TSb in Scheme 4) with less basic pyridines to a frontside attack (TSf in Scheme 4) with more basic pyridines.[7]

In the present work of the pyridinolysis of **1**, the authors propose a stepwise mechanism with a rate-limiting step change from bond breaking with more basic pyridines to bond formation with less basic pyridines based on: (i) the considerably large β_X = 1.98 with the stronger nucleophiles and small β_X = 0.22 with the weaker nucleophiles, as observed in **2S** where β_X(**2S**) = 1.36-1.50 and 0.23-0.48 with the stronger and weaker nucleophiles, respectively; (ii) the relatively small enthalpy of activation and large negative entropy of activation ($\Delta H^{\ddagger}$ = 3.5 kcal mol^{-1} and $\Delta S^{\ddagger}$ = –63 cal mol^{-1} K^{-1}), as observed in **2S** ($\Delta H^{\ddagger}$ = 6.4 kcal mol^{-1} and $\Delta S^{\ddagger}$ = –53 cal mol^{-1} K^{-1}); and (iii) biphasic concave upward free energy relationship with X, as observed in **2S**. Biphasic concave upward free energy relationship for substituent X variations in the nucleophiles are ascribed to a change in the attacking direction of the nucleophile from a frontside (TSf) with more basic pyridines to a backside (TSb) with less basic pyridines.

The attacking direction of the nucleophile changes from a frontside to a backside as the nucleophile becomes less basic for both the anilinolysis and pyridinolysis. However, there is the difference between the anilinolysis and pyridinolysis regarding the mechanism: (i) in the anilinolysis, a concerted mechanism regardless of the attacking direction; (ii) in the pyridinolysis, a stepwise process with a rate-limiting bond breaking involving a frontside attack whereas with a rate-limiting bond formation involving a backside nucleophilic attack.[11]

Experimental Section

Materials. Bis(2-oxo-3-oxazolidinyl) phosphinic chloride and HPLC grade acetonitrile (water content < 0.005%) were used without further purification. Anilines were redistilled or recrystallized before use. Deuterated anilines were synthesized as reported earlier.[2,3] Pyridines were used without further purification.

Kinetic Procedure. Rates and selectivity parameters were obtained as previously described for the anilinolysis[2,3] and pyridinolysis.[6,7] Initial concentrations for both the anilinolysis and pyridinolysis were as follows; [substrate] = 5 × 10^{-3} M and [nucleophile] = (0.10-0.30) M.

Product Analysis. In the case of the anilinolysis, bis(2-oxo-3-oxazolidinyl) phosphinic chloride was reacted with excess aniline for more than 15 half-lives at 55.0 °C in MeCN. The aniline hydrochloride salt was separated by filtration. Solvent was removed under reduced pressure. The product was isolated through treatment with ether and dilute HCl by a work up process and then dried over $MgSO_4$. After filtration the product was isolated by evaporating the solvent under reduced pressure. In the case of the pyridinolysis, bis(2-oxo-3-oxazolidinyl) phosphinic chloride was reacted with excess pyridine, for more than 15 half-lives at 35.0 °C in MeCN. Solvent was removed under reduced pressure. The product was isolated by adding ether and insoluble fraction was collected. The product was purified to remove excess pyridine by washing several times with ether and MeCN. The analytical and spectroscopic data of the products gave the following results (see Supporting Information):

[$C_6H_8N_2O_4P$(=O)NHC_6H_5]: White solid crystal; mp 204-205 °C; ^{1}H-NMR (400 MHz, MeCN-d_3) δ 3.92-3.97 (m, 4H), 4.32-4.40 (m, 4H), 6.88-6.90 (m, 1H), 7.05-7.32 (m, 5H); ^{13}C-NMR (100 MHz, MeCN-d_3) δ 45.43, 65.04, 118.39, 120.08, 123.87, 130.51, 174.11; ^{31}P-NMR (162 MHz, MeCN-d_3) δ 3.57 (1P, s, P=O); GC-MS (EI, *m/z*) 311 (M^+).

[($C_6H_8N_2O_4$)P(=O)NC_5H_5]$^+$Cl$^-$: White solid crystal; mp 131-132.0 °C; ^{1}H-NMR (400 MHz, D_2O) δ 3.98-4.02 (m, 4H), 4.41-4.50 (m, 4H), 8.12-8.83 (m, 5H); ^{13}C-NMR (100 MHz, D_2O) δ 45.7, 64.8, 126.2, 127.6, 156.9, 160.0, 173.4, 180.0; ^{31}P-NMR (162 MHz, D_2O) δ 3.77 (1P, s, P=O) ; LC-MS for $C_{11}H_{13}N_3O_5PCl$ (EI, *m/z*), 333 (M^+).

Acknowledgments. This work was supported by Inha University Research Grant.

References and Notes

1. (a) Lee, I. *Chem. Soc. Rev.* **1990**, *19*, 317. (b) Lee, I. *Adv. Phys. Org. Chem.* **1992**, *27*, 57. (c) Lee, I.; Lee, H. W. *Collect. Czech. Chem. Commun.* **1999**, *64*, 1529.
2. Guha, A. K.; Lee, H. W.; Lee, I. *J. Chem. Soc., Perkin Trans. 2* **1999**, 765.
3. (a) Hoque, M. E. U.; Dey, S.; Guha, A. K.; Kim, C. K.; Lee, B. S.; Lee, H. W. *J. Org. Chem.* **2007**, *72*, 5493. (b) Hoque, M. E. U.; Dey, N. K.; Kim, C. K.; Lee, B. S.; Lee, H. W. *Org. Biomol. Chem.* **2007**, *5*, 3944. (c) Dey, N. K.; Hoque, M. E. U.; Kim, C. K.; Lee, B. S.; Lee, H. W. *J. Phys. Org. Chem.* **2009**, *22*, 425. (d) Hoque, M. E. U.; Guha, A. K.; Kim, C. K.; Lee, B. S.; Lee, H. W. *Org. Biomol. Chem*. **2009**, *7*, 2919. (e) Hoque, M. E. U.; Lee, H. W. *Bull. Korean Chem. Soc.* **2012**, *33*, 663. (f) Barai, H. R.; Lee, H. W. *Bull. Korean Chem. Soc.* **2012**, *33*, 1037.
4. (a) Poirier, R. A.; Wang, Y.; Westaway, K. C. *J. Am. Chem. Soc.* **1994**, *116*, 2526. (b) Yamata, H.; Ando, T.; Nagase, S.; Hanamura, M.; Morokuma, K. *J. Org. Chem*. **1984**, *49*, 631. (c) Zhao, X. G.; Tucker, S. C.; Truhlar, D. G. *J. Am. Chem. Soc*. **1991**, *113*, 826.
5. (a) Melander, L., Jr.; Saunders, W. H. *Reaction Rates of Isotopic Molecules*; Wiley-Interscience: New York, 1980. (b) Lee, I.; Koh, H. J.; Lee, B. S.; Lee, H. W. *J. Chem. Soc., Chem. Commun.* **1990**, 335. (c) Marlier, J. F. *Acc. Chem. Res*. **2001**, *34*, 283. (d) Westaway, K. C. *Adv. Phys. Org. Chem*. **2006**, *41*, 217.
6. Guha, A. K.; Lee, H. W.; Lee, I. *J. Org. Chem*. **2000**, *65*, 12.
7. Hoque, M. E. U.; Dey, S.; Kim, C. K.; Lee, H. W. *Bull. Korean Chem. Soc*. **2011**, *32*, 1138.
8. Taking into account the anilinolysis rate ratio of k_H(**2**)/k_H(**1**) = 1.26 at 55.0 °C, the pyridinolysis rate of **2** is exceptionally fast. Moreover, the pyridinolysis rate of **2** is unusually fast compared to the rates of other (R_1O)(R_2O)P(=O)Cl-type substrates where R_1 and R_2 are alkyl or aryl.
9. (a) Hondal, R. J.; Bruzik, K. S.; Zhao, Z.; Tsai, M. D. *J. Am. Chem. Soc.* **1997**, *119*, 5477. (b) Holtz, K. M.; Catrina, I. E.; Hengge, A. C.; Kantrowitz, E. R. *Biochemistry* **2000**, *39*, 9451. (c) Omakor, J. E.; Onyido, I.; vanLoon, G. W.; Buncel, E. *J. Chem. Soc., Perkin Trans. 2* **2001**, 324. (d) Gregersen, B. A.; Lopez, X.; York, D. M. *J. Am. Chem. Soc.* **2003**, *125*, 7178. (e) Onyido, I.; Swierczek, K.; Purcell, J.; Hengge, A. C. *J. Am. Chem. Soc*. **2005**,

127, 7703. 324. (f) Liu, Y.; Gregersen, B. A.; Hengge, A. C.; York, D. M. *Biochemistry* **2006**, *45*, 10043.

10. All the ρ_{XY} values were calculated with twelve second-order rate constants and the correlation coefficients for *b*- (r = 0.980), *c*- (r = 0.981) and *d*-block (r = 0.935) are not tolerable. The signs of ρ_{XY} can be acceptable, although the magnitudes of ρ_{XY} values are not fully acceptable. In general, more than twenty rate constants are employed to minimize the error.
11. The authors cannot completely neglect a concerted mechanism with less basic pyridines, because the nonlinear free energy correlation of a concave upward plot is generally interpreted as diagnostic of a change in the reaction mechanism, while nonlinear free energy correlation of a concave downward plot as diagnostic of a rate-limiting step change from bond breaking with less basic nucleophiles to bond formation with more basic nucleophiles. The authors dare to say that this is not an 'iron law' but general.